

# Evaluating Solar Energy Harvesting using Artificial Neural Networks: A Case study in Togo

Koffi Agbeblewu Dotche  
Department of Electrical Engineering,  
Ecole Nationale Supérieure d'Ingénieurs  
(ENSI),  
University of Lome,  
Lomé- Togo  
E-mail : kdotche2004@gmail.com

Adekunlé Akim Salami  
Department of Electrical Engineering,  
Ecole Nationale Supérieure d'Ingénieurs  
(ENSI),  
University of Lome,  
Lomé-Togo  
E-mail : akim\_salami@yahoo.fr

Koffi Mawugno Kodjo  
Department of Electrical Engineering,  
Ecole Nationale Supérieure d'Ingénieurs  
(ENSI),  
University of Lome,  
Lomé-Togo  
E-mail : rig\_kodjo@yahoo.fr

Yawa Pamela C. D. BLU  
Department of Electrical Engineering,  
Institut de Formation Technique Supérieur (IFTS),  
Lomé, TOGO

Yao Essemu Julien DIABO  
Department of Electrical Engineering,  
Institut de Formation Technique Supérieur (IFTS),  
Lomé, TOGO  
E-mail:juliendiabo@yahoo.fr

**Abstract**--The work sought to develop a model for the evaluation of solar energy harvesting potentials in Togo using an approach based on artificial neural networks (ANNs) in order to predict the daily irradiation for some areas under climatic conditions. Two types of ANN architecture were evaluated the radial basic function (RBF) and multi-layer perceptron (MLP). The data were collected in 28 cities, and data from of 8 cities were used for the training stage in order to come with the suitable model for the other cities. The results indicated that the ANN-MLP model 8 has provided the best performance and its accuracy was tested. Furthermore, the solar generation potential was evaluated. The sites in the study have exhibited a high potential for solar energy generation.

**Index Terms**-- artificial neural networks; modelling energy harvesting; solar irradiance prediction

## I. INTRODUCTION

Energy is an essential factor in the socio-economic development of a modern society. However, the constant exploitation of fossil energy sources causes pollution of our planet [1]. The exploration of new sources of non-polluting energy is essential and the world is interested in clean renewable energy sources such as solar, wind, hydroelectric and biomass, to avoid the accelerated destruction of the ozone layer and to meet the worldwide energy demand. The energy consumption of Togo is increasing year after year, forcing the country to import more than 75% of its electricity consumption in 2010 and about 85% in 2015 [2]. In this scope, the Togolese government has adopted a program to harvest the solar energy over a period of 2015 to 2030. This aims at covering around the 60% of the domestic electricity demand of the inhabitants of its localities. It is undeniably mastering the production of solar photovoltaic energy, will require the deep knowledge of solar irradiation at the point of deploying this solar micro-grid. In this quest, some measurements of solar irradiation are often performed but the measuring exercise itself is very expensive; and to which come along the problems such as the calibration

from the measuring devices, lack of maintenance of the measuring sensors. In regard to these problems, some empirical models were developed [3] and others based on artificial intelligence to estimate solar irradiation relying on some meteorological data such as ambient temperature, relative humidity, sunshine, cloud etc. and geographical data such as longitude, altitude and latitude. Recently, artificial neural networks have been used to get a high accuracy in deep learning and stood as a universal approximation tool in prediction. They have found great application in the forecast of energy demand, and many more. For example, Alsina et al., [3] have developed an optimal neural model to predict the monthly average of global solar irradiance daily in 45 localities in Italy. The performances obtained through the statistical indicators have shown that the obtained model displayed a high accuracy in the estimation of the monthly average of the daily global solar irradiation in Italy. In [4], the wind speed was predicted while investigating the wind energy potential on the Lome's site by using an artificial neural network. In [5], [6] the authors have also used the artificial neural network for the forecast of energy demand.

This study departed from the [4] and [6]. It sought to develop a model for the estimation of solar irradiance values in Togo using an approach based on artificial neural networks (ANNs) under climatic conditions. In this scope, this will help in reducing the costs that will be incurred when measuring the daily availability of solar irradiation data on each site. The data were collected in 28 cities, some part of these data were used for the training stage in order to come with the suitable model that was tested in the other cities.

## II. THE MODEL

In this section the modelling using the artificial neural network is announced.

### A. The artificial neural network architecture

In neural network the nodes behave like in a typical mesh node on the principle of forward and move on. Each neuron or node forward its signal to the next node. Two kinds of signals are used, the function and errors signals.

- The function signals (also called input signals) that come in at the input of the network, propagate forward (neuron by neuron) through the network and reach the output end of the network as output signals;
- The error signals that originate at the output neuron of the network and propagate backward (layer by layer) through the network.

The ANN multi-layer perceptron (MLP, see Figure 1) neural network and the radial basic function (RBF, see Figure 2) neural network architectures are the common used. The difference between the two is the function signal. The general output of the ANN is described by:

$$y = F_0 \left( \sum_{j=0}^M w_{0,j} \left( F_h \left( \sum_{i=0}^N w_{j,i} x_i \right) \right) \right) \quad (1)$$

where:

- $w_{oj}$  represents the synaptic weights from neuron  $j$  in the hidden layer to the single output neuron,
- $x_i$  represents the  $i^{\text{th}}$  element of the input vector,
- $F_h$  and  $F_0$  are the activation function of the neurons from the hidden layer and output layer, respectively,
- $w_{ji}$  are the connection weights between the neurons of the hidden layer and the inputs.

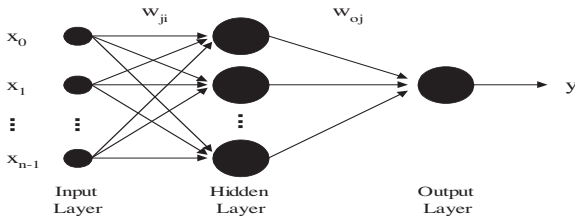


Figure 1. Configuration of the MLP

The radial basic function neural network architecture is given in Figure 2.

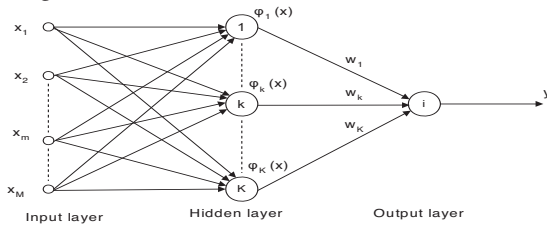


Figure 2. RBF-NN architecture

### B. Performance evaluation keys

The performance of each configuration was outweighed using the statistical figures such as the mean absolute percentage error (MAPE), root mean square error (RMSE), and correlation coefficient ( $R^2$ ). These are succinctly introduced.

#### 1. Mean absolute percentage error (MAPE)

The MAPE shows the mean absolute percentage difference between the predicted values and those attained by measured values, which is expressed as:

$$MAPE = \frac{1}{N} \sum_{i=1}^N \left| \frac{y_i - x_i}{y_i} \right| \cdot 100 \quad (2)$$

#### 2. Root mean square error (RMSE)

The RMSE identifies the model accuracy by comparing the deviation between the values achieved by the predicted values

and those of measured data. The RMSE has always a positive value given as:

$$RMSE = \sqrt{\frac{1}{N} \sum_{i=1}^N (y_i - x_i)^2} \quad (3)$$

### 3. Correlation coefficient ( $R^2$ )

The  $R^2$  indicates the strength of the linear relationship between the predicted values and the measured. It is computed as:

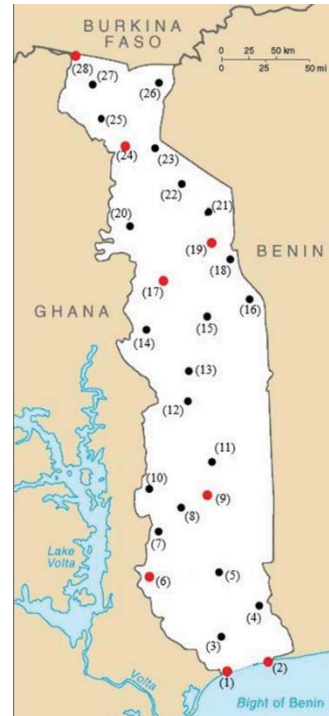
$$R^2 = \frac{\sum_{i=1}^N (x_i - \bar{x}_i)(y_i - \bar{y}_i)}{\sqrt{\sum_{i=1}^N (x_i - \bar{x}_i)^2 \sum_{i=1}^N (y_i - \bar{y}_i)^2}} \quad (4)$$

## III. METHODOLOGY AND RESEARCH INSTRUMENTS

The procedures of coming out with the best model under the climatic conditions are explained in this section.

### A. The data collection

The data sets were gathered over a span length of 5 years on a total of 28 localities. They contained the daily global irradiation values from January 2000 to June 2005. These different localities where the measurements were carried out for the modelling of the best neural network are depicted on the Map.



Amlamé	(8)
Aného	(2)
Anié	(11)
Atakpamé	(9)
Badou	(10)
Bafilo	(18)
Bassar	(17)
Blitta	(12)
Cinkassé	(28)
Danyi	(7)
Dapaong	(27)
Djarkpanga	(14)
Gando	(23)
Guérin-	
Kouka	(20)
Kantè	(22)
Kara	(19)
Kpalimé	(6)
Lomé	(1)
Mandouri	(26)
Mango	(24)
Niamtougou	(21)
Notsè	(5)
Sokodé	(15)
Sotouboua	(13)
Tabligbo	(4)
Tandjouaré	(25)
Tchamba	(16)
Tsévié	(3)

Figure 3. The sites of the study

### B. Data sampling and filtering

The data were divided into two. The 8 red dot sites indicated those that were selected for the learning stage and validation for the remained sites.

### C. The system configuration

The input parameters are described in Table I and the various configuration accordingly to the meteorological data are given in the Table II.

TABLE I : DESCRIPTION OF THE INPUTS PARAMETERS

Type	Input relevance	Symbol	Unit
Meteorology	Mean of air Temperature	Tmean	°C
	Maximum of air Temperature	Tmax	°C
	Difference	$\Delta T$	°C
	Atmospheric pressure	Patm	kPa
	Mean relative humidity	Hu	%
	Insolation duration	( $S_0$ )	minut
Astronomic	Declinaison	( $\delta$ )	Degree celsius (°)
Astronomic		( $\omega_0$ )	Degree celsius (°)
	Altitude		
	Latitude		
	Longitude		
Time span	Number of month	Nmonth	1 to 12

TABLE II : THE INPUTS VARIABLES TO THE MODELS

Mo del	Input Variables										
	$\delta$	$S_0$	$\omega_0$	Pa tm	T mo y	$\Delta T$	T ma x	Hu m.	Lo ng.	La lt.	A lt.
1	X	X	X	X	X	X	X	X	X	X	X
2					X	X	X	X	X	X	X
3		X	X	X	X	X	X	X	X	X	X
4	X		X	X	X	X	X	X	X	X	X
5	X	X		X	X	X	X	X	X	X	X
6	X	X	X		X	X	X	X	X	X	X
7			X	X	X	X	X	X	X	X	X
8				X	X	X	X	X	X	X	X
9	X	X			X	X	X	X	X	X	X
10		X		X	X	X	X	X	X	X	X
11		X	X		X	X	X	X	X	X	X
12	X		X		X	X	X	X	X	X	X

Mo del	Input Variables										
	$\delta$	$S_0$	$\omega_0$	Pa tm	T mo y	$\Delta T$	T ma x	Hu m.	Lo ng.	La lt.	A lt.
13	X			X	X	X	X	X	X	X	X
14	X				X	X	X	X	X	X	X
15		X			X	X	X	X	X	X	X
16			X		X	X	X	X	X	X	X

## IV. RESULTS AND DISCUSSION

This section provides the obtained results, and discusses their relevancy.

The results that are obtained by the usage of the ANN-RBF have displayed the same trend, however a maximum MAPE about 5% was recorded as shown in Figure 4.

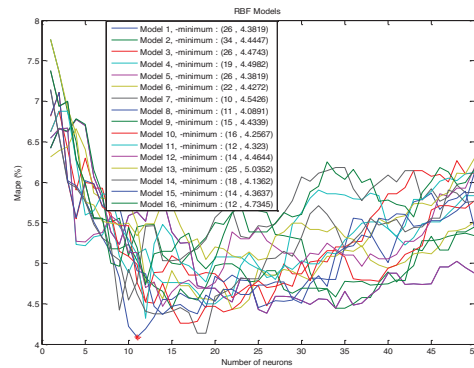


Figure 4: The RBF models

Meanwhile, all the configurations using the MLP also produce the same trend, but in this case a maximum MAPE about 3.8% is recorded as shown in Figure 5.

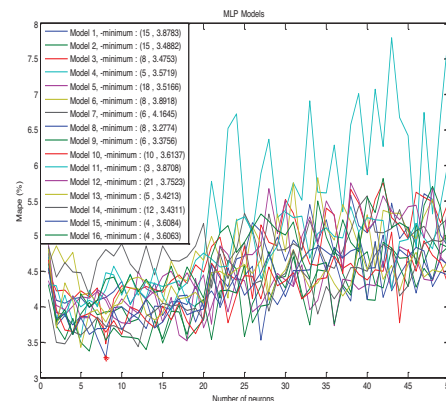


Figure 5: The MLP models

The analysis of the trained models, is indicating that the MAPE has a mean value around 5.4369% and the  $R^2$  has a value 0.9 for the RBF configuration; meanwhile for the MLP's configuration MAPE with a maximal value about 3.80% ,

having an  $R^2$  about 0.92 for the MLP, slightly higher than that of the RBF.

After the training stage, the model configuration that had the high performance was selected, in this study, the ANN-MLP, the model 8 has given the best performance. This model 8, was applied to the remained sites that were not considered in the training stage. The different errors obtained on each site are given in Table V.

TABLE III : STATISTICAL INDEX OF THESE MODELS FOR THE ANN- MLP

ANN-Multi Layer Perceptron				
Model	NB° of neurons	MAPE (%)	RMSE	$R^2$
1	15	3.8783	0.2492	0.9247
2	15	3.4882	0.2306	0.9328
3	8	3.4753	0.2343	0.9295
4	5	3.5719	0.2269	0.9323
5	10	3.4954	0.2294	0.9292
6	4	3.7876	0.2453	0.9192
7	2	3.7903	0.2412	0.9276
8	8	3.2774	0.2163	0.9332
9	6	3.3756	0.2160	0.9293
10	10	3.6137	0.2327	0.9312
11	3	3.8708	0.2507	0.9231
12	6	3.8497	0.2476	0.9148
13	5	3.4213	0.2246	0.9250
14	12	3.4311	0.2351	0.9207
15	6	3.6096	0.2370	0.9362
16	2	3.8072	0.2490	0.9147

TABLE IV : STATISTICAL INDEX OF THESE MODELS

Model	Radial Basis Function (RBF)			
	NB° of neurons	MAPE (%)	RMSE	$R^2$
1	19	4.5700	0.2861	0.9070
2	16	4.9872	0.3208	0.8616
3	26	4.4743	0.2910	0.9023
4	19	4.4982	0.2836	0.9036
5	26	4.3819	0.2760	0.9080
6	22	4.4272	0.2774	0.9098
7	10	4.5426	0.2934	0.8946
8	11	4.0891	0.2671	0.9123
9	15	4.4339	0.2799	0.9028
10	16	4.2567	0.2683	0.9162
11	12	4.3230	0.2951	0.8793
12	14	4.4644	0.2820	0.9062
13	25	5.0352	0.3345	0.8635
14	18	4.1362	0.2588	0.9079
15	18	4.3746	0.2801	0.9047
16	12	4.7345	0.2958	0.8944

With respect to the cities, a higher value around 9% and the lowest value of the correlation was about 0.85; it is therefore assumed that the derived model can be implemented to serve as a benchmark of the solar irradiation estimation in Togo.

TABLE V : STATISTICAL VALUES FOR TESTING

Cities	Statistical Parameters			
	MAPE (%)	NRMSE (%)	RMSE	$R^2$
Amlamé	7.8581	8.6300	0.4357	0.9368
Anié	5.3335	6.0794	0.3157	0.9176
Badou	8.2863	9.0570	0.4573	0.9325
Bafilo	5.9210	6.7641	0.3629	0.9106
Blitta	5.1249	6.1001	0.3228	0.9216
Danyi	4.6829	5.4362	0.2823	0.9084
Dapaong	3.6492	4.5964	0.2553	0.8991
Djarkpanga	9.1420	9.8577	0.5010	0.9143
Gando	3.5278	4.4484	0.2471	0.9045
Guérin-Kouka	5.0042	5.7675	0.3105	0.9140
Kantè	4.7670	5.5730	0.3061	0.9107
Mandouri	3.5775	4.4960	0.2497	0.9031
Niamtougou	6.3064	7.1807	0.3852	0.9019
Notsè	6.0019	7.0258	0.3496	0.8560
Sokodé	5.6131	6.6036	0.3494	0.9122
Sotouboua	5.6131	6.6036	0.3494	0.9122
Tabligbo	4.6311	5.7512	0.2862	0.8610
Tandjouaré	3.6492	4.5964	0.2553	0.8991
Tchamba	5.9210	6.7641	0.3629	0.9106
Tsévié	4.1282	5.4036	0.2689	0.8605
Total	5.4369	6.4390	0.3398	0.8855

The predicted values against the measured values are given in Figure 6, where a comparison chart is illustrated. The results have shown agreement with the forecasted data in [2]. Furthermore, the predicted harvesting energy on an inclined surface of 1 meter square using the photovoltaic farm in a near future are illustrated in Figure 7.

## V. CONCLUSION

This study aims at coming out with a model of estimating the solar irradiance values in Togo using an approach based on artificial neural networks (ANNs). The extent is to predict the daily irradiation for areas under climatic conditions where it is challenging to perform some measurement. Two ANN models were evaluated, the radial basic function and multi-layer perceptron. The training stage results have indicated that the MAPE and the  $R^2$  have a mean value about 5.4369% and 0.9 respectively for the ANN-RBF configuration; meanwhile that

of ANN-MLP, the MAPE has a maximal value about 3.8 and the  $R^2$  about 0.92 for the MLP. The model configuration 8, of ANN-MLP has achieved the best performance amongst. In addition, the comparative results of the selected model with respect to the cities, has shown a highest MAPE value around 9%, which is less than 10%; and the lowest value of the correlation  $R^2$  was about 0.85. The study has achieved very significant results and the sites in the study have exhibited a high potential for solar energy generation. Further research should be directed into the a-priori deployment of solar farms in the country based on the cloud computing technology.

## REFERENCES

- [1] International Energy Agency, 2008: *Energy Technology Perspectives: Strategies and Scenarios to 2050*. Paris.
- [2] NASA, 2018. *Meteorology and Solar Radiation site*. [online] Available at: <https://eosweb.larc.nasa.gov/cgi-bin/sse/retscreen.cgi?email=rets%40nrcan.gc.ca&step=1&lat=-30.503&lon=29.364&submit=Submit>

- [3] Emmanuel Federico Alsina, Marco Bortolini, Mauro Gamberi, and Alberto Regattieri, Artificial neural network optimization for monthly average daily global radiation prediction, Elsevier Journal of Energy Conversion and Management, 120 (2016) pp. 320-329.
- [4] Salami Adekunle Akim, Ajavon Ayite senah Akoda, Prediction of the mean wind speed on the lome's site by neural networks (Prediction de la moyenne horaire de la vitesse du vent sur le site de Lomé par réseau de neurones), Revue du comes, Vol. 2(1) 2017, pp. 1-12
- [5] Mohamed M. Ismail and M. A. Moustafa Hassan, Artificial Neural Network Based Approach Compared with Stochastic Modelling for Electrical Load Forecasting, In Proceeding of the international Conference On Modelling Identification and control, Cairo-Egypt, 31stAugust -2<sup>nd</sup> Sept. 2013, pp.112-118.
- [6] A. Akim Salami, A. Sénah A. Ajavon, Koffi A. Dotche and Koffi-Sa Bedja, Electrical Load Forecasting Using Artificial Neural Network: The Case Study of the Grid Inter-Connected Network of Benin Electricity Community (CEB), American Journal of Engineering and Applied Sciences, Vol. 11 (2), April 2018, pp.471-481.

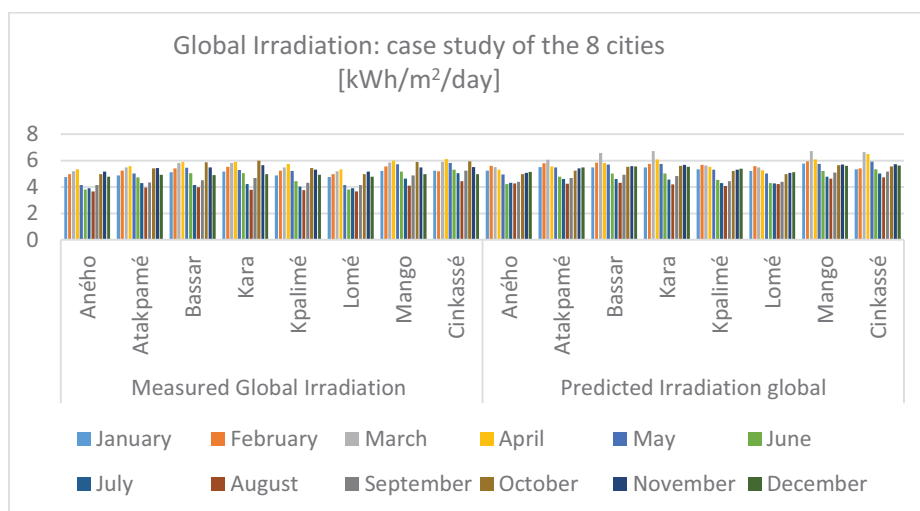


Figure 6: Comparison between the predicted and the measured solar irradiation

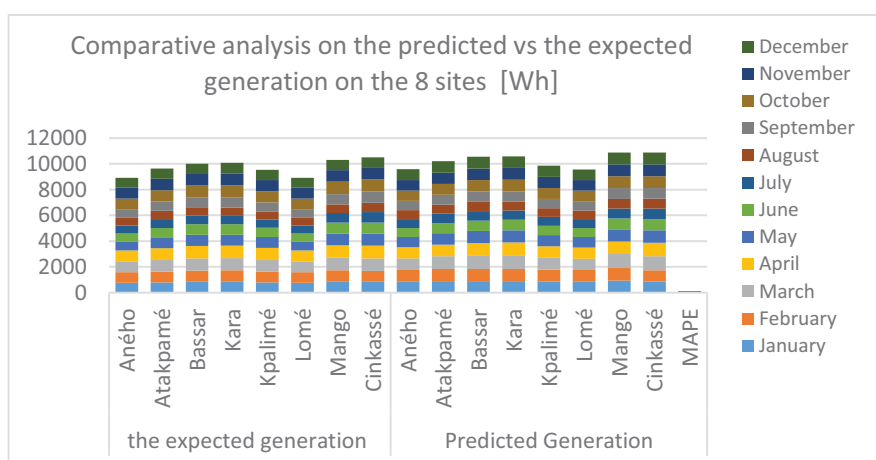


Figure 7: Comparison between the predicted and the measured generation